Wide dynamic range detection of bidirectional flow in Doppler optical coherence tomography using a two-dimensional Kasai estimator

Darren Morofke and Michael C. Kolios

Department of Physics, Ryerson University, Toronto, Canada

I. Alex Vitkin

Ontario Cancer Institute/University Health Network, Toronto, Canada

Victor X. D. Yang

Imaging Research, Sunnybrook Health Sciences Center, Toronto, Canada

We demonstrate extended axial flow velocity detection range in a time-domain Doppler optical coherence tomography (DOCT) system using a modified Kasai velocity estimator with computations in both the axial and transverse directions. For a DOCT system with an 8 kHz rapid-scanning optical delay line, bidirectional flow experiments showed a maximum detectable speed of >56 cm/s using the axial Kasai estimator without the occurrence of aliasing, while the transverse Kasai estimator preserved the ~ 7 μm/s minimum detectable velocity to slow flow. By using a combination of transverse Kasai and axial Kasai estimators, the velocity detection dynamic range was over 100 dB. Through a fiber-optic endoscopic catheter, *in vivo* *M*-mode transesophageal imaging of the pulsatile blood flow in rat aorta was demonstrated, for what is for the first time to our knowledge, with measured peak systolic blood flow velocity of >1 m/s, while maintaining good sensitivity to detect aortic wall motion at <2 mm/s, using this 2D Kasai technique. © 2007 Optical Society of America

OCIS codes: 170.3880, 170.4500, 110.4500, 170.3340, 170.2150, 100.2000.

Optical coherence tomography (OCT) can acquire of high-resolution images of subsurface tissue structure and function.[1–4] By use of autocorrelation,[5,6] phase sensitive detection,[7,8] and a Kasai velocity estimator,[9,10] Doppler frequency shifts can now be estimated in real time with Doppler OCT (DOCT). Flow velocity can be determined via phase detection with high sensitivity.[6–10] The transverse Kasai (TK) autocorrelation estimator is suitable for imaging slow bidirectional flows representative of microcirculation. Aliasing due to the axial scan (a-scan) frequency, however, limits the maximum TK detected nonaliased axial flow speed to <4 mm/s in OCT where rapid scanning optical delay (RSOD) lines operate at 8 to 15 kHz.[7,10,11] This upper limit is increased to ~ 8 mm/s on spectral domain[8] or swept-source OCT systems[12] with higher effective a-scan rates. New swept-source systems[13,14] with effective a-scan rates of 115 to 290 kHz can theoretically have an aliasing limit of 7 cm/s. Phase-unwrapping techniques can extend the velocity detection range; however, at high flow rates, separation between aliasing rings can become smaller than the spatial resolution of the imaging system, making phase unwrapping unreliable. Digital hardware autocorrelation with time delays less than the a-scan period[5] and Hilbert transform techniques[15] can provide higher aliasing limits up to ~ 35 cm/s with reduced sensitivity to low flow speed. However, in applications such as coronary imaging, flow velocity estimation in the range of meters per

second is required. In addition, blood flow velocity in the microvasculature of atheroma can be orders of magnitude lower than that in the lumen and both can be present in the OCT field of view.

In this Letter we report Kasai autocorrelation performed in both the axial and transverse directions, on the same data set, which results in an extended axial velocity estimation range. It is based on the 2D Kasai algorithm proposed by Loupas *et al.*[16] for ultrasound imaging. We previously reported TK estimation of flow-induced frequency shift.[10] The aliasing limits are $\pm 1/2f_a$, the a-scan frequency, which is typically in the kilohertz range. Sampling rate in the axial direction, however, is in the megahertz range. To take advantage of the larger bandwidth, we propose the axial Kasai (AK) algorithm, computed as

$$f_{\text{AK}} = \frac{f_s}{2\pi} \tan^{-1} \frac{\sum_{m=0}^{M-2} \sum_{n=0}^{N-1} (Q_{m,n} I_{m+1,n} - I_{m,n} Q_{m+1,m})}{\sum_{m=0}^{M-2} \sum_{n=0}^{N-1} (I_{m,n} I_{m+1,n} + Q_{m,n} Q_{m+1,n})}, \quad (1)$$

where f_s is the sampling rate and provides the aliasing limits at $\pm 1/2f_s$. I and Q are in-phase and quadrature components of the signal, and m and n are the axial and transverse indices. When a stationary AK result is subtracted from a moving source, the remaining signal is the Doppler shift induced by the

motion of the scatterers. The change in frequency is related to velocity by $v = \lambda_0 \Delta f / 2 n_t \cos \theta$, where v is the velocity at a specific point, λ_0 is the center wavelength of the light, n_t is the refractive index of the sample, θ is the Doppler angle, and Δf is the change in frequency due to Doppler shift estimated by TK or moving AK subtracted from the stationary AK.

A flow phantom experiment was performed using an infusion pump with calibrated flow rate control and 1% Intralipid fluid pumped through a glass capillary 0.5 mm inner diameter at a Doppler angle of $\theta = 59°$. Images were acquired using a previously described time-domain DOCT system[10] containing a 5 mW broadband light source centered at 1.3 μm with 63 nm bandwidth with an 8 Hz a-scan frequency (f_a). Transverse Kasai variance (TKV) processing,[10] which computed the variance of the estimated mean Doppler shift, provided segmentation between flow and no-flow regions, similar to standard deviation Doppler imaging.[7] Stationary background AK phase change was then subtracted for AK flow visualization. The fastest experimentally achievable peak flow velocity was 2 m/s, with a Reynolds number of 730. The calculated entrance length was 13 mm, shorter than the capillary tube used. Laminar parabolic flow was assumed for all flow rates in this experiment. Different flow speeds were analyzed using Eq. (1), and the AK frequency results were shown in Fig. 1A. Bidirectional velocity was obtained by subtraction of the stationary signal, shown in Fig. 1B. The estimated peak velocities from the AK and TK (mean and standard deviation over 1000 lines) were plotted in Fig. 2, which showed good agreement between the measured and expected velocities. We separated the flow regimes into Zone I, with velocities estimated by TK; Zone II, where the spatial dimensions of the aliasing rings are larger than the spatial resolution of the system and phase unwrapping can be reliably applied; and Zone III, where TK aliasing rings are smaller than the axial resolution and the TKV approaches f_a; so phase unwrapping cannot be reliably performed, and the velocity estimation relies on AK, as shown in Fig. 3. In Zones I and II, the TK exhibited better velocity resolution than AK. Beyond them, the phase unwrapped TK underestimated the true velocities, where the AK was still able to estimate velocities with good agreement with set flow rates. Hence it is possible to use the full 2D Kasai estimator (TK and AK) to accurately measure across a wide
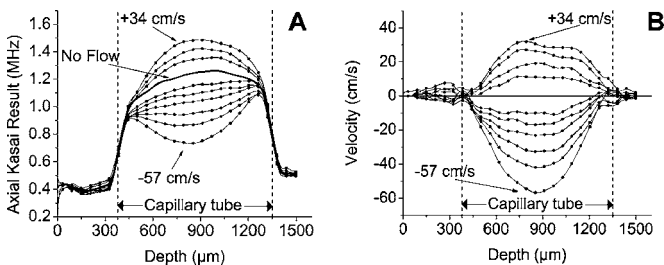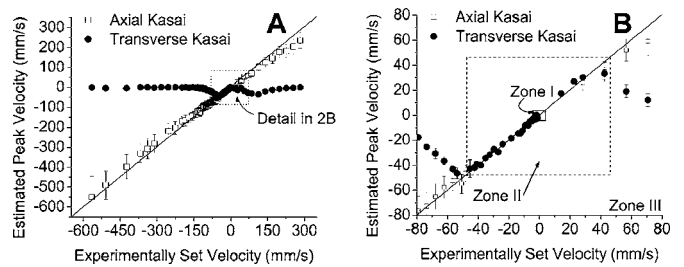
Fig. 2. TK and AK estimated peak velocities (mean and SD) are compared to expected flow velocities. A, Peak velocities derived from TK and AK algorithms recorded over a large range of velocities. B, detailed view of TK (with phase unwrapping) and AK estimated velocities for lower flow velocities. See text for Zone I, II, and III definitions.
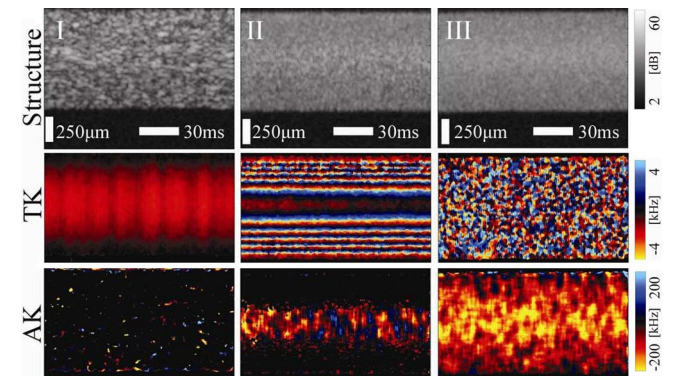
Fig. 3. (Color online) M-mode images of the three detection zones showing structural, TK, and AK color maps after flow segmentation. In (I), TK accurately measures velocity, and the aliasing rings in (II) can be unwrapped reliably. In (III), the aliasing rings cannot be accurately unwrapped. The AK is able to accurately measure flow in (III), but not in (I) and (II). Aggregation of Intralipid produced artifacts, especially at low shear rate regions.

range of flow velocities, spanning from (7 μm/s to ±57 cm/s, which is over 100 dB.

In vivo transesophageal M-mode DOCT imaging of a rat aorta was performed using an endoscopic catheter.[17] Motion artifacts were removed by a-scan alignment using the aortic wall to blood interface. The heart rate to be 230 beats per min or 0.26 s per beat. A temporal smoothing filter set at 0.025 s in length ($<$10% of the cardiac cycle), was used to improve the signal-to-noise ratio (SNR) while still preserving the temporal resolution and allowing visualization of the cardiac cycle. The Doppler angle was approximately 82°. The peak systolic velocity through the aorta was estimated to be $\sim$1 m/s (Fig. 4C), in good agreement with literature.[18] Comparing Figs. 4A and 4B, it is evident that the TK is sensitive to a slower flow, detecting the pulsating motion of the aortic wall (velocity $<$2 mm/s), while the AK is capable of estimating high flow velocities ($>$1 m/s) without aliasing. We are exploring the use of TKV to aid merging of the TK and AK results to yield a single wide dynamic range velocity image.

The physical limiting factor in the maximum detectable Doppler shift using AK in our system is the bandwidth of the hardware demodulation circuit, which is ±1.6 MHz ($-$3 dB point) around the carrier frequency. Since this is much smaller than the sam-

Fig. 1. A, Change in the AK estimated frequency as a function of flow velocities from $-$57 to 34 cm/s in capillary tube. B, When the no-flow AK result is subtracted from the flowing conditions, parabolic profiles are obtained.
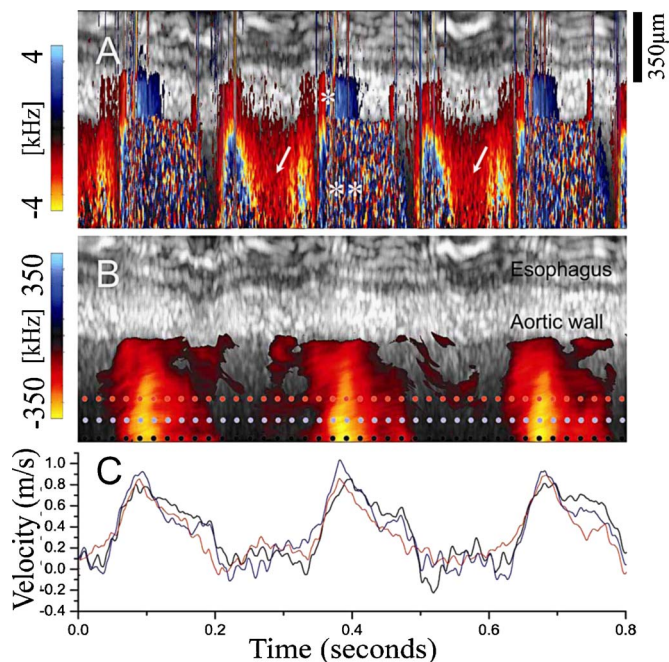
Fig. 4. (Color online) *In vivo M*-mode images of transesophageal DOCT of rate aortic blood flow. A, TK results overlaid on structural image. Doppler signals indicate aortic wall motion (∗), systolic rush of high-speed blood flow (∗∗), and regions of slow flow between heart beats (white arrows). B, AK results overlaid on the same structural image, with the esophagus and aortic wall labeled. High-speed systolic flow regions consistent with large Doppler frequency shifts are clearly visualized. The temporal flow profiles measured at the dotted lines of corresponding colors in B are plotted in C.

pling frequency of the system, the AK velocity estimator does not experience aliasing before the OCT signal diminishes. This corresponds to a maximum detectable velocity limit of ±0.78 m/s in the axial direction (±5.6 m/s at 82° with our endoscopic catheter), which can be further increased by widening the demodulation bandwidth, with a trade-off in SNR of the OCT signal. The computational complexity of AK is of the same order as TK and can be implemented for real-time operation in software.[10] Compared with previous autocorrelation methods,[5,6] the Kasai estimation output is linear with the flow velocity. We note that misalignments in the RSOD, wavelength-dependent scattering and absorption, and nonlinearities in the demodulation process contributed to the background AK phase changes, which need to be subtracted for visualizing the true flow induced phase changes. The TK and TKV processed from the same data set are sensitive to slow flow conditions, and the results can serve as segmentation maps for distinguishing stationary versus flow regions in subsequent AK calculations. Conversely, we are also exploring the AK as a tool for estimating the centroid shift due to wavelength-dependent scattering and absorption in spectroscopic OCT after the segmentation process.

In conclusion, we described the AK algorithm as a method for extending the velocity estimation range on high-speed DOCT systems, to include higher flow velocities. Using the Kasai autocorrelation technique in two dimensions by combining the AK with TK, one can obtain sensitivity from extremely slow to fast flow velocities on the same data set. For what is for the first time to our knowledge, we demonstrated *in vivo* transesophageal imaging of the rat aortic blood flow using the 2D Kasai technique.

References

1. D. Huang, E. A. Swanson, C. P. Lin, J. S. Schuman, W. G. Stinson, W. Chang, M. R. Hee, T. Flotte, K. Gregory, C. A. Puliafito, and J. G. Fujimoto, Science **254**, 1178 (1991).
2. X.-J. Wang, T. E. Milner, Z. Chen, and J. S. Nelson, Appl. Phys. Lett. **36**, 144 (1997).
3. Z. Chen, T. E. Miller, D. Dave, and J. S. Nelson, Opt. Lett. **22**, 64 (1997).
4. J. A. Izatt, M. D. Kulkarni, S. Yazdanfar, J. K. Barton, and A. J. Welch, Opt. Lett. **22**, 1439 (1997).
5. A. M. Rollins, S. Yazdanfar, J. K. Barton, and J. A. Izatt, J. Biomed. Opt. **7**, 123 (2002).
6. V. Westphal, S. Yazdanfar, A. M. Rollins, and J. A. Izatt, Opt. Lett. **27**, 34 (2002).
7. Y. Zhao, Z. Chen, C. Saxer, S. Xiang, J. F. de Boer, and J. S. Nelson, Opt. Lett. **25**, 114 (2000).
8. B. White, M. Pierce, N. Nassif, B. Cense, B. Park, G. Tearney, B. Boumma, T. Chen, and J. de Boer, Opt. Express **11**, 3490 (2003).
9. V. X. D. Yang, M. L. Gordon, A. Mok, Y. Zhao, Z. Chen, R. S. C. Cobbold, B. C. Wilson, and I. A. Vitkin, Opt. Commun. **208**, 209 (2002).
10. V. X. D. Yang, M. L. Gordon, B. Qi, J. Pekar, S. Lo, E. Seng-Yue, A. Mok, B. C. Wilson, and I. A. Vitkin, Opt. Express **11**, 794 (2003).
11. A. L. Oldenburg, J. J. Reynolds, D. L. Marks, and S. A. Boppart, Appl. Opt. **42**, 22 (2003).
12. B. J. Vakoc, S. H. Yun, J. F. de Boer, G. J. Tearney, and B. E. Bouma, Opt. Express **13**, 14 (2005).
13. R. Huber, M. Wojtkowski, and J. G. Fujimoto, Opt. Express **14**, 8 (2006).
14. W. Y. Oh, S. H. Yun, G. J. Tearney, and B. E. Bouma, Opt. Lett. **30**, 23 (2005).
15. A. W. Schaefer, J. J. Reynolds, D. L. Marks, and S. A. Boppart, IEEE Trans. Biomed. Eng. **51**, 186 (2004).
16. T. Loupas, J. T. Powers, and R. W. Gill, Ferroelectr. Freq. Control **42**, 672 (1995).
17. V. X. D. Yang, M. L. Gordon, S. J. Tang, N. E. Marcon, G. Gardiner, B. Qi, S. Bisland, E. Seng-Yue, S. Lo, J. Pekar, B. C. Wilson, and I. A. Vitkin, Opt. Express **11**, 19 (2003).
18. A. B. Driss, J. Benessiano, P. Poitevin, B. I. Levy, and J. B. Michel, Am. J. Physiol. Heart Circ. Physiol. **227**, 851 (1997).